Clustering of Redundant Parameters for Fault Isolation with Gaussian Residuals ⋆

Alexander Mendler * **Michael Döhler** ** **Carlos E. Ventura** *
Laurent Mevel **

* *Dept. of Civil Engineering, University of British Columbia, Vancouver BC, V6T 1Z4, Canada (e-mail: alexander.mendler@ubc.ca, ventura@civil.ubc.ca).*
** *Univ. Gustave Eiffel, Inria, COSYS/SII, I4S, 35042 Rennes, France (e-mail: michael.doehler@inria.fr, laurent.mevel@inria.fr)*

Abstract: Fault detection and isolation in stochastic systems is typically model-based, meaning fault-indicating residuals are generated based on measurements and compared to equivalent mathematical system models. The residuals often exhibit Gaussian properties or can be transformed into a standard Gaussian framework by means of the *asymptotic local approach*. The effectiveness of the fault diagnosis depends on the model quality, but an increasing number of model parameters also leads to redundancies which, in turn, can distort the fault isolation. This occurs, for example, in structural engineering, where residuals are generated by comparing structural vibrations to the output of digital twins. This article proposes a framework to find the optimal parameter clusters for such problems. It explains how the optimal solution is a compromise, because with an increasing number of clusters, the fault isolation resolution increases, but the detectability in each cluster decreases, and the number of false alarms changes. To assess these factors during the clustering process, criteria for the *minimum detectable change* and the *false-alarm susceptibility* are introduced and evaluated in an optimization scheme.

Keywords: Fault isolation, stochastic dynamic system, sensitivity matrix, over-parametrization

1. INTRODUCTION

There is an ongoing interest in developing fault diagnosis methods for safety-critical structures under operational loads, e.g. lifeline infrastructure, power plants, aircrafts and spacecrafts. To achieve robustness toward unknown input variations and changing operating conditions, many fault diagnosis methods are model-based but modelling large-scale systems and contrasting them with limited measurement data can result in an over-parametrization. As a result, not all parameters are identifiable and a small amount of noise can lead to great inaccuracies (Walter and Pronzato, 1990). As discussed by Chu and Hahn (2009), such problems can be found in the mathematical modeling of biological or biochemical systems, chemical reactions, ecological systems, power systems, production systems, and wastewater treatment systems. The basic problem is that the measured output is sensitive to changes in any parameter but it cannot be identified which parameter caused the deviation because multiple parameters exhibit similar sensitivities. To remedy this, a subset of parameters is chosen where sensitivity-based selection techniques include the collinearity index method (Brun et al., 2001), the column-pivoting method (Velez-Reyes and Verghese, 1995), an extension of the relative gain array (Sandink et al., 2001), the Gram-Schmidt orthogonalization (Yao et al., 2003), principal component analysis (Li et al., 2004), or the Fisher information matrix. Based on the latter, there are numerous ways to form optimization criteria, e.g. using its trace, its determinant (Weijers and Vanrolleghem, 1997), its singular values (Brun et al., 2002), or inverse (Walter and Pronzato, 1990). The parameter selection is usually advanced until the sensitivity matrix is of full rank, because then all parameters are identifiable.

For fault isolation in mechanical systems, damage-sensitive features are extracted from vibration data and contrasted with over-parametrized system models, e.g. finite element (FE) models. In FE model updating, e.g. a residual is established by confronting frequency and mode shape estimates with the mass and stiffness of FE models (Friswell and Mottershead, 2013). Swindlehust et al. (1995) confronted the observability matrix estimated from data with the one obtained from FE models. Basseville et al. (2004) employed a parametrized GLR test that includes the sensitivity toward selected FE parameters. To reduce redundancies, Balmès et al. (2008) and Allahdadian et al. (2019) proposed clustering approaches that combine parameters with similar sensitivities; however, without evaluating the pertinence of the achieved reduced parametrization. This article follows this line of work and proposes three physical criteria to find the optimal parameter cluster, which are the *fault isolation resolution*, the *minimum detectable change*, as well as the *false-alarm susceptibility*.

The paper is organized as follows: Section 2 introduces a formula for the minimum detectable change and recaps

⋆ The financial support from the Natural Sciences and Engineering Research Council of Canada (NSERC), the German Academic Exchange Service (DAAD) and the Mitacs Globalink Research Award is gratefully acknowledged.

the fault isolation based on the asymptotic local approach. Section 3 proposes the optimization criteria, and in Section 4, the approach is applied to the subspace-based residual for fault isolation on a pin-supported beam structure.

2. PROBLEM STATEMENT

We consider the problem of detecting and isolating changes in a system that is characterized by H parameters, stored in the vector $\theta \in \mathbb{R}^H$, with the selective system measurements $\mathcal{Y}_N = \{Y_1, \dots, Y_N\}$ being the realization of an asymptotically stationary process. The local approach (Benveniste et al., 1987) assumes the close hypotheses

$$\begin{aligned} \mathbf{H}_0 &: \ \theta = \theta^0 && \text{(reference system)}, \\ \mathbf{H}_1 &: \ \theta = \theta^0 + \delta/\sqrt{N} && \text{(faulty system)}, \end{aligned} \tag{1}$$

where δ is unknown but fixed. We regard a residual vector $\zeta(\theta^0, \mathcal{Y}_N)$ that satisfies the central limit theorem (CLT)

$$\zeta \longrightarrow \begin{cases} \mathcal{N}(0, \Sigma) & \text{under } \mathbf{H}_0 \\ \mathcal{N}(\mathcal{J}\delta, \Sigma) & \text{under } \mathbf{H}_1 \end{cases}. \tag{2}$$

Herein, $\mathcal{J} \in \mathbb{R}^{l \times H}$ is the residual's sensitivity toward parameter changes, and $\Sigma \in \mathbb{R}^{l \times l}$ is its covariance. Based on (2), fault detection and isolation can be carried out in a standard Gaussian framework (Döhler et al., 2016).

2.1 Fault Detectability

Change detection in the residual (2) is carried out by testing $\delta = 0$ against $\delta \neq 0$, which amounts to the GLR (Basseville et al., 2000)

$$t = \zeta^T \Sigma^{-1} \mathcal{J} \left(\mathcal{J}^T \Sigma^{-1} \mathcal{J} \right)^{-1} \mathcal{J}^T \Sigma^{-1} \zeta. \tag{3}$$

The resulting test statistic follows a χ^2-distribution with $\text{rank}(F)$ degrees of freedom and non-centrality $\lambda = \delta^T F \delta$, where $F \in \mathbb{R}^{H \times H}$ is the Fisher information matrix

$$F = \mathcal{J}^T \Sigma^{-1} \mathcal{J}. \tag{4}$$

Assuming a change in a single parameter θ_h (as the h-th component of θ), the non-centrality writes

$$\lambda_h = F_{hh} \delta_h^2. \tag{5}$$

To analyze the detectability of changes in θ_h, λ_h needs to exceed some value $\lambda_{\min}$, which can be calculated based on the accepted false-alarm rate α as well as the allowable false-positive rate β, see Fig. 1. Solving (5) for δ_h and plugging it into (1) for a fixed N results in

$$\theta_h - \theta_h^0 \approx \sqrt{\frac{\lambda_{\min}}{N \cdot F_{hh}}} \tag{6}$$

which is a formula for the minimum change in a single parameter θ_h that can be detected reliably. Mendler et al. (2019) originally developed this formula for fault detection and this paper extends the theory to fault isolation.

2.2 Fault Isolation

Testing parameters individually for changes, i.e. $\delta_h = 0$ against $\delta_h \neq 0$, can be done analogously to (3) in the *direct test* or *sensitivity test* (Döhler et al., 2016)

$$t_h = \zeta_h^T F_{hh}^{-1} \zeta_h, \qquad \zeta_h = \mathcal{J}_h^T \Sigma^{-1} \zeta, \tag{7}$$

where $\mathcal{J}_h$ is the h–th column of the Jacobian. The parameter with the greatest test response is likely to be the faulty one. Unfortunately, fault-free parameters also show

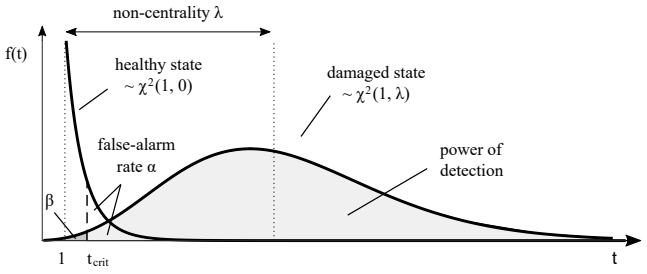

Fig. 1. χ^2- distribution with one DOF

a response due to the off-diagonal terms of the Fisher information matrix in (7). They can be diminished through the *minmax test* as follows. The Jacobian is rearranged $\mathcal{J} = [\mathcal{J}_h \mathcal{J}_{\bar{h}}]$ and the Fisher information is organized as

$$F = \begin{bmatrix} F_{hh} & F_{h\bar{h}} \\ F_{\bar{h}h} & F_{\bar{h}\bar{h}} \end{bmatrix} = \begin{bmatrix} \mathcal{J}_h^T \Sigma^{-1} \mathcal{J}_h & \mathcal{J}_h^T \Sigma^{-1} \mathcal{J}_{\bar{h}} \\ \mathcal{J}_{\bar{h}}^T \Sigma^{-1} \mathcal{J}_h & \mathcal{J}_{\bar{h}}^T \Sigma^{-1} \mathcal{J}_{\bar{h}} \end{bmatrix}, \tag{8}$$

where h is the tested partition and $\bar{h}$ the complementary one. After defining the partial residuals

$$\zeta_h = \mathcal{J}_h^T \Sigma^{-1} \zeta, \ \zeta_{\bar{h}} = \mathcal{J}_{\bar{h}}^T \Sigma^{-1} \zeta, \tag{9}$$

a robust residual and its Fisher information can be formed through orthogonal projections (Döhler et al., 2016)

$$\zeta_h^* = \zeta_h - F_{h\bar{h}} F_{\bar{h}\bar{h}}^{-1} \zeta_{\bar{h}}, \quad F_h^* = F_{hh} - F_{h\bar{h}} F_{\bar{h}\bar{h}}^{-1} F_{\bar{h}h}, \tag{10}$$

preserving the residual's sensitivity toward changes in the tested partition and making it blind to changes in the untested partition. The corresponding distribution is

$$\zeta_h^* \sim \mathcal{N}(F_h^* \delta_h, F_h^*). \tag{11}$$

Ultimately, the minmax test statistic is given by

$$t_h^* = \zeta_h^{*T} F_h^{*-1} \zeta_h^*, \tag{12}$$

which is χ^2-distributed with one degree of freedom and non-centrality $\lambda_h = \delta_h^T F_h^* \delta_h$.

2.3 Hierarchical Parameter Clustering

The problem addressed in this paper is that this fault isolation approach is not applicable to problems with a (nearly) rank deficient Fisher information. Rank deficiency could be caused by an over-parametrization, i.e. problem formulations where multiple parameters have similar sensitivities toward the residual. Consequently, linear dependencies arise in the columns of the Jacobian matrix and a basic condition for the projection in (10) is violated. As a remedy, Balmès et al. (2008) proposed a k-means-based clustering approach, which was later replaced by Allahdadian et al. (2019) through a hierarchical clustering, where redundant parameters are combined in a new parametrization. Herein, the first step is to define

$$\tilde{\mathcal{J}} = \Sigma^{-1/2} \mathcal{J} = \begin{bmatrix} \tilde{\mathcal{J}}_1 & \cdots & \tilde{\mathcal{J}}_H \end{bmatrix} \tag{13}$$

for consistency with (3) and (4). Secondly, the cosine between the vectors is used to measure the dissimilarity

$$d_{ij} = 1 - \frac{\tilde{\mathcal{J}}_i^T \tilde{\mathcal{J}}_j}{||\tilde{\mathcal{J}}_i|| \cdot ||\tilde{\mathcal{J}}_j||}.$$

If the two vectors are orthogonal, the cosine is one and the dissimilarity is zero. If the two vectors are linearly dependent, the value is one. After evaluating the distances d_{ij}, they can be ranked in descending order. At the start of the first iteration, the number of clusters K equals the number of parameters H. For each iteration, the distances

between all pairs of clusters are evaluated according to the complete-linkage cluster distance, defined as (Duda et al., 2012)

$$D(C_a, C_b) = \max\{d_{ij} : i \in C_a, j \in C_b\}.$$

Gradually, the two clusters with the shortest distance $d = \min\{D(C_a, C_b) : a \neq b\}$ are combined, until only one cluster is left so $K = 1$. For each K, the cluster centres c_k can be determined through averaging as

$$c_k = \frac{1}{m_k} \sum_{i \in C_k} \tilde{\mathcal{J}}_i,$$

where m_k is the number of parameters in cluster C_k and $k \in [1, \ldots, K]$ is the cluster number. Finally, the cluster centres are arranged in the clustered Jacobian $\mathcal{J}^c = [c_1 \cdots c_K]$. The expression $k(h)$ is the cluster number of the cluster $C_{k(h)}$ that contains parameter θ_h. When applying the test to parameter θ_h according to (8)–(12), the untested partition $\Sigma^{-1/2}\mathcal{J}_{\bar{h}}$ in (8) and (9) is replaced by the cluster centres of the clusters that do not contain θ_h, so

$$\mathcal{J}^c_{\bar{h}} = \begin{bmatrix} c_1 & \ldots & c_{k(h)-1} & c_{k(h)+1} & \ldots & c_K \end{bmatrix}. \tag{14}$$

Hierarchical clustering has several advantages in comparison to other approaches, such as k-means. For example, convergence is guaranteed regardless of the starting point (Allahdadian et al., 2019). However, a disadvantage is that the number of clusters needs to be defined, by setting a cut-off value d_{trim} for the dissimilarity up to which clusters are combined. That means that it is up to the user to define a sufficient degree of separability. This is where the current paper comes into play, as it proposes a generalized approach to find the optimal number of parameter clusters.

3. OPTIMAL PARAMETER CLUSTERING

This section presents three criteria for an optimal parameter clustering, i.e. the fault isolation resolution, the minimum detectable change and the susceptibility to false alarms in the fault isolation. Furthermore, the section outlines how each criterion can be weighted by proposing both an upper and a lower bound and how an optimal cut-off value d_{trim} can be found as a compromise between all three objective functions $f_1 - f_3$ through Pareto optimization.

3.1 Fault Isolation Resolution

The first and most intuitive optimality criterion is the fault isolation resolution. It can be quantified through the number of clusters, i.e. the number of columns in the Jacobian matrix $\mathcal{J}^c$, because each cluster can individually be tested for faults. The higher the number of clusters, the higher the resolution. When formulated as a minimization problem, the corresponding objective function writes

$$f_1(K) = \frac{K - K_b}{K_g - K_b}, \tag{15}$$

where K is the number of clusters and g and b are indices for a good and bad number of clusters, respectively. Fault isolation with a single cluster is meaningless, which is why the lower bound for the number of clusters should be set to $K_b = 2$. The upper bound could, for example, be set to the maximum number of distinguishable parameters, so $K_g = \text{rank}(F)$. The objective function in (15) yields zero if the number of clusters is equal to the optimal number of substructures, and one for $K_b = 2$.

3.2 Minimum Detectable Change

Another optimality criterion is the minimum detectable change for each individual parameter θ_h. It can be estimated by exchanging the Fisher information in (6) with its robust equivalent in (10) after clustering,

$$\Delta_h(K) = \frac{\theta_h - \theta^0_h}{\theta^0_h} \approx \frac{1}{\theta^0_h} \sqrt{\frac{\lambda_{min}}{N \cdot F^{*c}_h}}, \tag{16}$$

where $F^{*c}_h = F^{*c}_h(K)$ with $F^{*c}_h = F_{hh} - F^c_{h\bar{h}} F^{c-1}_{\bar{h}\bar{h}} F^c_{\bar{h}h}$ with $F^c_{h\bar{h}} = \tilde{\mathcal{J}}^T_h \mathcal{J}^c_{\bar{h}}$ and $F^c_{\bar{h}\bar{h}} = \tilde{\mathcal{J}}^{cT}_{\bar{h}} \tilde{\mathcal{J}}^c_{\bar{h}}$, see (13) and (14). With the normalization by the nominal value θ^0_h, it is possible to define a hard upper bound of 100%. A lower minimum detectable change corresponds to higher detectability. If multiple parameters are monitored simultaneously, the decisive parameter is the one with the highest minimum detectable change. Following this train of thought, an objective function can be defined as

$$f_2(K) = \frac{\Delta_{\max}(K) - \Delta_g}{\Delta_b - \Delta_g}, \tag{17}$$

where $\Delta_{\max}(K) = \max\{\Delta_1(K), ..., \Delta_H(K)\}$ from (16), and Δ_g and Δ_b are the user-defined lower and upper bounds. Our recommendation is to use $\Delta_g = 0\%$ as the ideal solution, and $\Delta_b = 100\%$ as the upper physical bound. The objective function could then be simplified to $f_{2,a}(K) = \Delta_{\max}(K)$ which yields values greater than one if faults cannot be detected reliably.

3.3 False Alarms in the Fault Isolation

The third optimality criterion is the number of parameters $\theta_{h'}$, $h' \in \{1, \ldots, H\}$, which, when faulty, would lead to false alarms. A false alarm in the fault isolation is understood as a considerable response of the test for parameters in fault-free clusters. To ease the interpretation of the following notations, it should be recalled that parameters are tested against cluster centres in this paper, cf. (13) and (14).

The problem originates in the projection from (10) which can lead to errors when the Fisher information is badly conditioned. For each h', let the parameter $\theta_{h'}$ be the only faulty parameter and $\delta = \delta'$ be the corresponding change vector. The h'–th component $\delta'_{h'}$ is non-zero, while all other entries of δ' are zero. This single fault scenario corresponds to hypothesis $\mathbf{H}'_1 : \theta = \theta^0 + \delta'/\sqrt{N}$. When testing any θ_h for a fault while $\theta_{h'}$ is faulty, the mean of the robust residual in (11) should be zero when θ_h is not in the same cluster as $\theta_{h'}$, i.e. with $k(h) \neq k(h')$, by design of the test. However, this cannot be guaranteed when the Fisher information is badly conditioned, and it is dependent on the number of clusters and the cluster centres.

The proposed approach to analyze such false alarms is the numerical computation of the theoretical non-centrality parameter of the test (12), which should be zero for the fault-free parameters θ_h with $k(h) \neq k(h')$. Under the respective δ', the expected value of the robust residual is computed based on (8)–(11) as follows. It holds that $\mathbf{E}(\zeta) = \mathcal{J}\delta' = \mathcal{J}_{h'}\delta'_{h'}$ and thus, under $\mathbf{H}'_1$,

$$\mathbf{E}(\zeta_h) = \mathcal{J}^T_h \Sigma^{-1} \mathcal{J}_{h'} \delta'_{h'} = F_{hh'} \delta'_{h'},$$
$$\mathbf{E}(\zeta_{\bar{h}}) = \mathcal{J}^{cT}_{\bar{h}} \Sigma^{-1/2} \mathcal{J}_{h'} \delta'_{h'} = \mathcal{J}^{cT}_{\bar{h}} \tilde{\mathcal{J}}_{h'} \delta'_{h'} = F^c_{\bar{h}h'} \delta'_{h'},$$

$$\begin{aligned}\mathbf{E}(\zeta_h^*) &= \mathbf{E}(\zeta_h) - F_{h\bar{h}}^c F_{\bar{h}\bar{h}}^{c-1}\mathbf{E}(\zeta_{\bar{h}}) \\ &= (F_{hh'} - F_{h\bar{h}}^c F_{\bar{h}\bar{h}}^{c-1} F_{\bar{h}h'}^c)\delta_{h'}'.\end{aligned}$$

Note that the last term should be zero for $k(h) \neq k(h')$ by design of the minmax test, if the parametrization (i.e. the clusters) is correctly defined. With the covariance F_h^{*c} of the robust residual, corresponding to (10), the non-centrality parameter of the test (12) under $\mathbf{H}_1'$ yields

$$\lambda_{h,h'} = (F_{hh'} - F_{h\bar{h}}^c F_{\bar{h}\bar{h}}^{c-1} F_{\bar{h}h'}^c)^2 \delta_{h'}'^2 / F_h^{*c},$$

which should be zero for any h with $k(h) \neq k(h')$. Note that for $h = h'$, $\lambda_{h',h'} = F_{h'}^{*c}\,\delta_{h'}'^2$. Therefore, the ratio

$$\lambda_{h,h'}/\lambda_{h',h'} = (F_{hh'} - F_{h\bar{h}}^c F_{\bar{h}\bar{h}}^{c-1} F_{\bar{h}h'}^c)^2 / (F_h^{*c} F_{h'}^{*c}) \quad (18)$$

predicts the relative reaction of the test for parameter θ_h while parameter $\theta_{h'}$ is faulty.

One way to formulate an objective function based on false alarms is to define a threshold for the relative magnitude of false alarms (18) in any fault-free parameter θ_h, with $k(h) \neq k(h')$, e.g. $1\% - 25\%$. If the threshold is exceeded for any θ_h, the parameter $\theta_{h'}$ is flagged as a false-alarm scenario. Then, an objective function can be defined as

$$f_3(K) = \frac{N_{sc}(K) - N_g}{N_b - N_g}, \quad (19)$$

with $N_{sc}(K)$ being the number of flagged parameters $\theta_{h'}$, $h' \in \{1, \ldots, H\}$ where the threshold is exceeded, and N_g and N_b are user-defined values that define the best and the worst cases. The total number of test scenarios equals the number of parameters, but our recommendation is to set $N_g = 0$ and $N_b = \gamma H$ with $\gamma = 0.5$ the maximal acceptable fraction of false-alarm-prone scenarios.

It occurs that some cluster configurations cause the false alarms to considerably exceed the safety threshold value. In a single-fault scenario, this makes it challenging to reliably isolate the fault, and masks faults in other parameters in a multi-fault scenario. It might even lead to false fault isolation results if the false alarm exceeds the test response of the actually faulty parameter. Hence, we recommend discarding such clusterings by introducing a second false-alarm threshold, e.g. $\bar{t}_{FA}^* = 50\%$.

3.4 A-posteriori Pareto Optimization

All criteria are considered equally, as fault detectability is equally important as the isolability, and fault isolation becomes meaningless if the number of false alarms is excessive. They all depend on the dendrogram distance d and the associated number of clusters K in the clustering approach. The lower the cut-off value d_{trim} is set, the higher the fault isolation resolution K and the smaller the detectability. The isolation resolution and the minimum detectable change are conflicting, because with an increasing number of clusters, the orthogonal projection in (10) has to be performed with respect to more non-tested cluster centres, which reduces the information content on tested parameters, and thus, the change detectability Δ. That means that neither of the two objective function can be improved without degrading the other. It may be possible to reduce the number of false alarms and one other objective at the same time, but the number of false alarms appears to be uncorrelated with the fault isolation resolution or the minimum detectable change.

Dealing with conflicting objective functions is known as *Pareto optimization*. In our case, all solutions are already given and the decision-making can be done a posteriori because evaluating the cluster tree and all three objective functions at all branches is completed in a matter of seconds. Several approaches have been proposed to deal with multi-objective decision-making. The most simple one is to reduce all three objectives to one by adding them up and applying appropriate weighting factors. Equivalently, a lower and upper bound could be chosen for each variable reducing each objective function to the feasible interval between zero and one, so $f_i \in [0, 1]$. Choosing lower and upper bounds is the preferred way in this paper because it has the same effect as weighting the objective functions but seems more intuitive for the problem at hand,

$$\begin{aligned}\min_K \quad & \mathcal{F} = \sqrt{f_1(K)^2 + f_2(K)^2 + f_3(K)^2} \\ \text{s.t.} \quad & f_1(K) < 1, f_2(K) < 1, f_3(K) < 1\end{aligned} \quad (20)$$

4. NUMERICAL APPLICATION

For proof of concept, the automated substructuring approach is applied to the stochastic subspace-based damage diagnosis (SSDD) of a pin-supported beam. The overall goal is to find an optimal parameter clustering for damage localization, meaning a configuration with a maximum number of substructures, a maximum fault detectability, as well as a minimum false alarm susceptibility.

4.1 Pin-supported HSS Beam

The 4.11 m-long pin-supported beam has a hollow structural steel section, HSS 152×51×4.78 mm, and a modulus of elasticity of 200.000 MPa. For modelling, the beam is split into 18 finite beam elements with a length of 22.8 cm each. The first six vertical modes of vibration are used to monitor the beam for faults with natural frequencies of $f_n = [8.97, 35.8, 80.3, 142, 220, 314]$ Hz and a modal damping ratio of 1% critical damping. For excitation, a uniformly distributed white noise excitation is applied at each of the 104 degrees of freedom. Four uni-axial sensors are placed along the beam, see Fig. 2, sampling the velocity in the vertical direction at a rate of 720 Hz. The measurement duration in the reference and testing state is set to 20 min and 25 s, respectively.

4.2 Residual Definition

The vibration behaviour of the structure can be modelled by a linear and time-invariant (LTI) mechanical system

$$\mathcal{M}\ddot{z}(t) + \mathcal{C}\dot{z}(t) + \mathcal{K}z(t) = w(t), \quad (21)$$

where $\mathcal{M}, \mathcal{C}, \mathcal{K} \in \mathbb{R}^{m\times m}$ are the mass, damping and stiffness matrices and $z(t) \in \mathbb{R}^m$ are displacements due to the random disturbances $w(t)$. Using vibration sensors, some components of z, $\dot{z}$ or $\ddot{z}$ can be measured in discrete-time. For signal processing, the model from (21) can be transformed to the discrete-time state space model

$$\begin{aligned}x_{\kappa+1} &= Ax_\kappa + w_\kappa \\ y_\kappa &= Cx_\kappa + v_\kappa.\end{aligned}$$

The model order is $n = 2m$ and the vectors $x_\kappa \in \mathbb{R}^n$ and $y_\kappa \in \mathbb{R}^r$ are the state vector and the measurement vector of all r outputs. $A \in \mathbb{R}^{n\times n}$ and $C \in \mathbb{R}^{r\times n}$ are the state

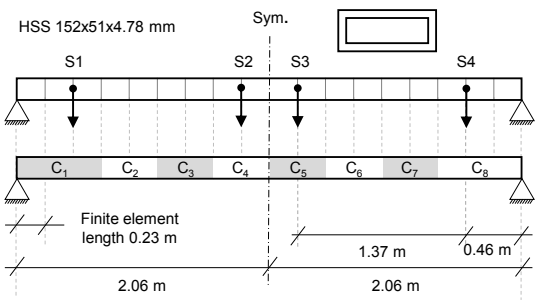

Fig. 2. Substructuring the pin-supported HSS beam

transition and the output matrices. The remaining terms $w_\kappa \in \mathbb{R}^n$ and $v_\kappa \in \mathbb{R}^r$ are white noise terms.

For residual generation, the output covariance estimates $\hat{R}_i = \frac{1}{N}\sum_{k=1}^{N} y_{\kappa+i} y_\kappa^T$ are computed, where $i \in \{1, \ldots, p+q\}$ with $\min(pr, qr) \geq n$, and arranged in block Hankel format $\hat{\mathcal{H}}_{p+1,q} = \text{Hank}(\hat{R}_i)_{i=1,\ldots,p+q}$. The Hankel matrix in the reference state yields the singular value decomposition

$$\hat{\mathcal{H}}^0_{p+1,q} = \begin{bmatrix}\hat{U}_1 & \hat{U}_0\end{bmatrix} \begin{bmatrix}\hat{D}_1 & 0 \\ 0 & \hat{D}_0 \approx 0\end{bmatrix} \begin{bmatrix}\hat{V}_1^T \\ \hat{V}_0^T\end{bmatrix}$$

and an asymptotically Gaussian residual results from the multiplication of the reference left null space $\hat{U}_0$ with the current Hankel matrix. The residual is defined as

$$\zeta = \sqrt{N}\text{vec}(\hat{U}_0^T \hat{\mathcal{H}}_{p+1,q}),$$

and satisfies the CLT (2) (Basseville et al., 2000). The Jacobian matrix is established by linking the residual to the stiffness parameter in $\mathcal{K} = \mathcal{K}(\theta^0)$, represented by the material stiffness of each FE, so here $\theta^0 = [E_1, ..., E_{18}]^T$, see (Basseville et al., 2004; Allahdadian et al., 2019).

4.3 Optimized Parameter Cluster

Following the recommendations in this paper, the threshold for the false alarms was set to 25% and 50%, and the maximum achievable number of clusters was evaluated by $K_g = \text{rank}(F) = 12$, see (15). The optimization process is visualized in Fig. 3 (a) where all three objective functions, i.e. the isolation resolution f_1 from (15), the minimum detectability f_2 from (17), and the false alarms susceptibility f_3 from (19) are shown together with the overall optimization metric $\mathcal{F}$ from (20).

For a better understanding, the 3-D Pareto frontier is plotted in 2-D, showing the isolation resolution over the minimum detectability and the false alarms, respectively, see Fig. 3 (b). Herein, the objective function $\mathcal{F}$ is the 3-D distance to the origin (dashed lines). The global minimum (solid line) occurs for eight parameter clusters $\{C_1, \ldots, C_8\}$ and the corresponding substructure arrangement is shown in Fig. 2. The decisive parameter for the minimum detectability is the FE right next to the support, as it exhibits the lowest Fisher information, and thus, the greatest minimum detectable change of $\Delta_1 = 15\%$.

The trade-off between fault detectability and isolation resolution appears to have a distinct optimum. This optimum point can be observed when plotting the minimum detectability f_2 over the number of parameter clusters f_1, see Fig. 3 (a), as it rapidly increases beyond 11 clusters. However, the alleged optimal point often exhibits a significant number of false-alarm scenarios, see f_3 in Fig. 3 (a), so the actual optimum is not at but close to this point. Here, the importance of the third objective function becomes clear. Although it is not necessarily conflicting with the other optimization criteria, meaning it is possible to improve the false-alarm susceptibility while improving one of the other objective functions as well, it should–in our opinion–be considered as an objective function in the optimization, and certainly as a knock-out criterion.

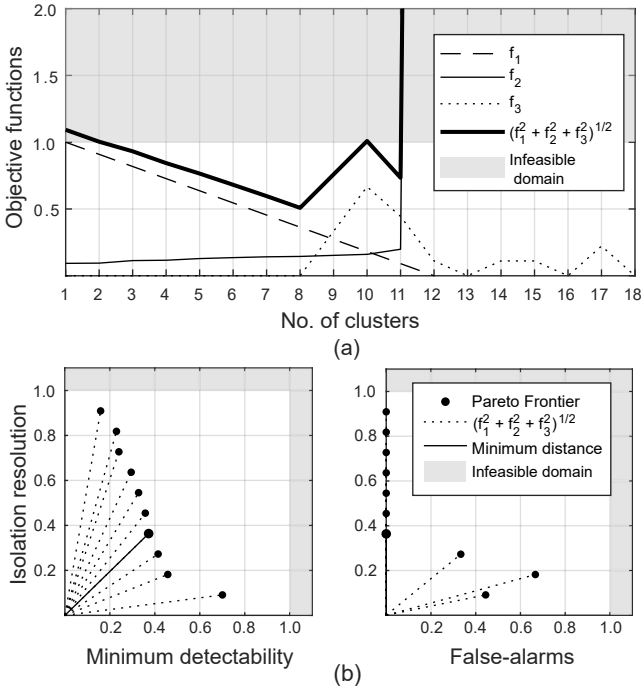

Fig. 3. (a) Optimization variables, and (b) Pareto frontier

4.4 Validating the Results

The validation of the minimum detectable change from (16) is visualized in Fig. 4, which shows the test response to a fault in the health parameter with the lowest minimum detectable change, i.e. parameter θ_1 in cluster C_1, see Fig. 2. To simulate the empirical test response to an actual fault, the modulus of elasticity in the model is reduced by $\Delta_1 = 15\%$ and the statistical test from (12) is applied to 100 data sets from the faulty structure. The minimum non-centrality was evaluated based on a maximum type I and II error of $\alpha = \beta = 2\%$. By looking at the test response for parameter θ_1 in Fig. 4, we can appreciate that the empirical false-positive rate is identical to the theoretical one $\beta_{emp} \approx \beta = 2\%$, meaning the prediction for the minimum detectable change is correct.

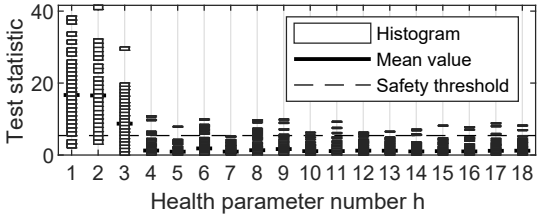

Fig. 4. Test response to a fault $\Delta_1 = 0.15$.

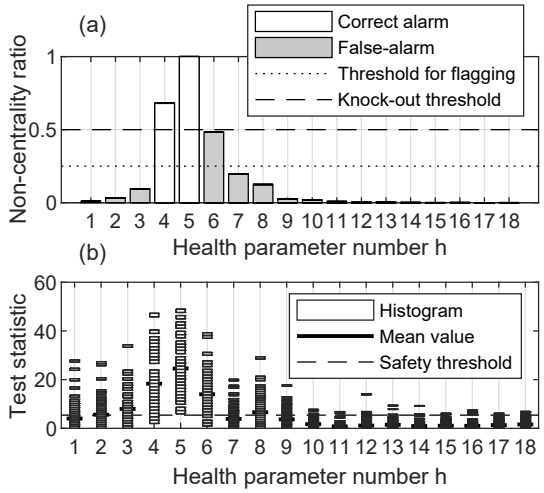

Fig. 5. Tests for faulty parameter number $h' = 5$. (a) Predicted test response (18), (b) actual one using (16).

To validate the false alarm prediction in (18), the empirical validation is repeated for faulty parameter number $h' = 5$ and juxtaposed to the prediction, see Fig. 5. Though less pronounced, the test for parameter θ_4 reacts beyond the safety threshold in both cases, as it is in the same cluster as θ_5. However, this case is flagged as a false-alarm scenario because the magnitude of the false alarm in parameter θ_6 (which is about 48%) exceeds the threshold of 25%, see Fig. 5 (a). The prediction is confirmed by the empirical test response in Fig. 5 (b), as the non-centrality of the empirical test for parameter θ_6 (the distance between one and the horizontal dash) is about half as large as for θ_5.

5. CONCLUSION

The results of this paper are clear evidence that parameter clustering in over-parametrized mechanical systems for fault isolation is a multi-objective optimization problem. One criterion is the minimum detectable change, which cannot exceed the physical limit of 100%. It is evaluated based on the Fisher information, which is related to the probability of detecting faults. Fault detectability does not guarantee isolability, because false alarms can obscure the actual fault location. For this reason, a second optimization criterion was developed that allows to predict false-alarms. Since both criteria can be evaluated based on data from the fault-free structure, they are also appropriate criteria for sensor placement optimization and should be considered in future work.

REFERENCES

Allahdadian, S., Döhler, M., Ventura, C., and Mevel, L. (2019). Towards robust statistical damage localization via model-based sensitivity clustering. *Mechanical Systems and Signal Processing*, 134, 106341.

Balmès, É., Basseville, M., Mevel, L., Nasser, H., and Zhou, W. (2008). Statistical model-based damage localization: a combined subspace-based and substructuring approach. *Structural Control and Health Monitoring*, 15(6), 857–875.

Basseville, M., Abdelghani, M., and Benveniste, A. (2000). Subspace-based fault detection algorithms for vibration monitoring. *Automatica*, 36(1), 101–109.

Basseville, M., Mevel, L., and Goursat, M. (2004). Statistical model-based damage detection and localization: subspace-based residuals and damage-to-noise sensitivity ratios. *Journal of Sound and Vibration*, 275(3-5), 769–794.

Benveniste, A., Basseville, M., and Moustakides, G. (1987). The asymptotic local approach to change detection and model validation. *IEEE Transactions on Automatic Control*, 32(7), 583–592.

Brun, R., Kühni, M., Siegrist, H., Gujera, W., and Reichert, P. (2002). Practical identifiability of asm2d parameters—systematic selection and tuning of parameter subsets. *Water research*, 36(16), 4113–4127.

Brun, R., Reichert, P., and Künsch, H.R. (2001). Practical identifiability analysis of large environmental simulation models. *Water Resources Research*, (37), 1015–1030.

Chu, Y. and Hahn, J. (2009). Parameter set selection via clustering of parameters into pairwise indistinguishable groups of parameters. *Industrial & Engineering Chemistry Research*, 48(13), 6000–6009.

Döhler, M., Mevel, L., and Zhang, Q. (2016). Fault detection, isolation and quantification from Gaussian residuals with application to structural damage diagnosis. *Annual Reviews in Control*, 42, 244–256.

Duda, R.O., Hart, P.E., and Stork, D.G. (2012). *Pattern classification*. John Wiley & Sons.

Friswell, M. and Mottershead, J.E. (2013). *Finite element model updating in structural dynamics*, volume 38. Springer Science & Business Media.

Li, R., Henson, M.A., and Kurtz, M.J. (2004). Selection of model parameters for off-line parameter estimation. *IEEE Transactions on Control Systems Technology*, 12(3), 402–412.

Mendler, A., Allahdadian, S., Döhler, M., Mevel, L., and Ventura, C. (2019). Minimum detectable damage for stochastic subspace-based methods. In *Proc. of IOMAC - International Operational Modal Analysis Conference*.

Sandink, C.A., McAuley, K.B., and McLellan, P.J. (2001). Selection of parameters for updating in on-line models. *Industrial & Engineering Chemistry Research*, 40(18), 3936–3950.

Swindlehust, A., Roy, R., Ottersten, B., and Kailath, T. (1995). A subspace fitting method for identification of linear state-space models. *IEEE Transactions on Automatic Control*, 40(2), 311–316.

Velez-Reyes, M. and Verghese, G.C. (1995). Subset selection in identification, and application to speed and parameter estimation for induction machines. In *Proceedings of International Conference on Control Applications*, 991–997. IEEE.

Walter, É. and Pronzato, L. (1990). Qualitative and quantitative experiment design for phenomenological models - a survey. *Automatica*, 26(2), 195–213.

Weijers, S.R. and Vanrolleghem, P.A. (1997). A procedure for selcting best identifiable parameters in calbrating activated sludge model no.1 to full-scale plant data. *Water science and technology*, 36(5), 69–79.

Yao, K.Z., Shaw, B.M., Kou, B., McAuley, K.B., and Bacon, D.W. (2003). Modeling ethylene/butene copolymerization with multi–site catalysts: Parameter estimability and experimental design. *Polymer Reaction Engineering*, 11(3), 563–588.